

ORIGINAL RESEARCH

The effects of soil-structure interaction in the seismic design of wind turbine foundations by investigating the impact of cement on soil: A case study of Firuz-Bahram soil

ZabihiSamani M.^{1*}, Esmacili Seyedmansouri Z.¹, Daryabari M.¹, Farhoud A.², GhanooniBagha M.³

Abstract:

In this paper, by presenting an applied model for simulating wind turbines with mat foundation and soil in an integrated manner, the effects of soil-structure interaction on the seismic behavior of wind turbines and the effect of soil stabilized with different percentages of cement have been studied. For this purpose, a new method for three-dimensional modelling of the rectangular cube foundation has been formulated and presented, assuming its rigid behavior. After importing the suggested model into the ABAQUS software, its adequacy and ability to reduce the time computation without decreasing the accuracy of the responses will be demonstrated. In this study, the effects of soil-structure interaction on the seismic response of 65-kW and 1-MW horizontal-axis wind turbine engines with conical steel towers have been investigated. The two proposed turbines with a mat foundation and frequency-based design have been analyzed. Likewise, the soil is first simulated as a spring to verify the accuracy of the output results. Then, the soil is modelled with the Mohr-Coulomb behavioral model in ABAQUS software, and the obtained results will be discussed and analyzed. It is worth bearing in mind that for verification, only the frequency outputs of the software were compared with the basic paper, and then the mesh dimensions and element boundary distances were examined for the study and software approval.

Keywords:

Wind turbine, seismic analysis, soil-structure interaction, soil stabilization with cement, natural frequency

✉*Corresponding author Email: Ma.zabihi@iau.ac.ir

1 Department of Civil Engineering, Pa.C., Islamic Azad University, Tehran, Iran

2 Civil Engineering Department, K.N. Toosi University of Technology, No. 1346, Tehran 19697, Iran

3 Department of Civil Engineering, ET.C., Islamic Azad University, Tehran, Iran

1. Introduction

One of the clean energy sources is wind. In recent decades, the desire to use this energy in the form of wind turbines has been increasing in most countries [1]. The decrease in the number of prime sites with good wind availability and accessibility, coupled with the increasing demand for higher output, has increased the need to use tall towers with long blades, especially on low-slope sites [2]. In seismically active areas, tall wind turbines generate large seismic forces, sometimes greater than the wind forces [3-4]. In such cases, an incorrect estimation of the seismic force can lead to failure or structural incompatibility. One of the important factors in estimating seismic forces in wind turbines is the interaction of soil, foundation and structure, which is affected by various parameters, including turbine size, foundation type and soil properties [5]. Another less studied topic is the seismic analysis of these structures under earthquake excitation. It is worth bearing in mind that until recent years, the main standards used for wind turbines did not provide any criteria for seismic analysis [6-7].

Initially, in 2006, a guideline entitled “Wind turbines: fundamentals, technologies, application, economics” [8] provided general recommendations. This guideline is considered as a basis for addressing the challenges related to seismic loading. A model for seismic analysis is proposed that considers the mass of the nacelle, the beam and a quarter section of the tower, and the mass concentrated at the tip of the tower. It is proposed that the obtained oscillation time be used to select a spectral response acceleration from the design response spectrum, which is used to determine the seismic loads on the tower [8]. In 2010, the “Guidelines for the Certification of Wind Turbines.” [9] provided little detail on earthquake engineering issues, unlike the previous guidelines [8].

These guidelines are more of a suggestion and provide recommendations for various seismic hazards. The guidelines first suggest that either local building codes be used or that

recommendations from the American Petroleum Institute [10] be used in consultation with J.L. Wind [11]. Details of the required seismic analyses are then presented. Lavasas et al. [12] performed a detailed finite element modelling of a 1-MW turbine with a 44 m steel tower and a 52 m diameter rotor, designed for installation in Greece. The seismic loading in this study was considered based on a linear analysis whose design response spectrum was selected from Eurocode 3 for seismic zone 2 with rocky soil. They found that the stresses due to earthquakes were 60% lower than those due to peak wind power. They then converted the model to a simple model with concentrated mass for the nacelle and the girder section at the tip of the tower; and observed that in areas with higher seismic hazard and poorer soil conditions, The design of the seismic may be decisive.

In 2021, Yan et al. conducted a buckling analysis of a 10 MW offshore wind turbine (OWT) subjected to wave, wind, and earthquake loading. The results show that wind and wave loads have a significant impact on the seismic responses of OWTs. Therefore, wind and wave loading cannot be ignored when performing OWT seismic analysis [13]. Lin et al. [14] conducted a study to investigate how soil and structure interaction affects the seismic performance of wind turbines. The results of this study showed that soil-structure interaction significantly affects the dynamic response of wind turbines.

The issue of soil-structure interaction as a phenomenon affecting the behaviour of structures has attracted the attention of structural engineers in recent years. Research shows that the effect of interaction on the seismic response of a structure compared to the response of a fixed foundation may increase or decrease, depending on the characteristics of the soil and structure [15-16]. Also, the type of soil under the structure is important for the analysis, design, evaluation, and improvement of buildings, so that failure to consider the type of soil in the analysis and design in the actual conditions of

the construction site can lead to a different level of performance compared to reality [17]. The effect of soil-structure interaction can change the natural frequency of the structure very close to the operating frequencies. Therefore, it is assumed that a fixed tower foundation in the design may be conservative but for a more optimal design soil-structure interaction analysis may be necessary [18-19-20]. In other words, to design wind turbine foundations, in addition to the bearing capacity of the soil, attention must also be paid to the dynamic characteristics of the wind turbine.

2. Materials and Methods

2-1- Project Soil Characteristics

In this study, the soil of the Firuz-Bahram area, located south of Azadegan Highway and east of Saveh Freeway, was used to investigate the effects of stabilization on soil. The soil of the studied area is classified as fine-grained clay (CL) with low plasticity

based on the suitable classification, and its characteristics and strength parameters were extracted from the paper by Zabihi Samani et al. [21].

2-2- Parts and material specifications

As mentioned at the beginning of this paper, two turbines i.e. 65-kW and 1-MW were used in this project. The specifications of these two wind turbines were extracted based on the 2017 paper by Austin et al. [5]. The table 2 summarizes the properties of the materials used in the model.

Two selected turbines i.e. 1-MW and 65-kW, have been used for this analysis. The blades in both turbines have three edges and are made of carbon fiber. Table 3 gives the exact dimensions of the two wind turbines used in this study. The dimensions of the soil and foundation of the structure are also extracted from the paper by Austin et al. [5] which are presented in Table 4. The detailed dimensions of the blades are also shown in Figure 1.

Table 1. Various soil parameters obtained from laboratory test [21]

Sample No.	Max Dry Density	OPT.Moisture Content	L.L	P.I	Remolded Sample		CBR	U.C.S	UU TEST		
	ASTM D 698				DRY Density	Moisture			5 mm	$\delta_3=(1.2.3 \text{ Kg/cm}^2)$	
	gr/cm ³	%			gr/cm ³	%				C	ϕ
Sample1	1.73	16	21	10	1.64	15.80	25	1.20	0.74	7.50	
3% cement+ sample1	1.75	15	17	7	1.66	14.90	33	1.35	0.76	7.60	
6% cement+ sample1	1.77	16	15	6	1.68	15.90	41	1.61	1.09	8.80	
8% cement+ sample1	1.81	15	12	5	1.66	17.50	71	2.80	1.61	10.70	

Table 2. Materials used in the turbine structure [5]

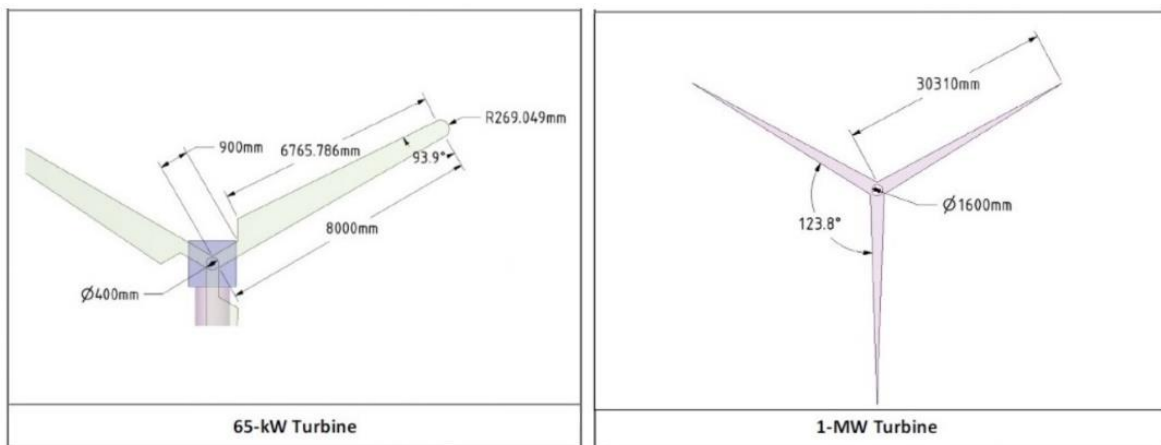
Property	Fiberglass and carbon fibers composite	Steel
Density	648 Kg/cm ³	7860 Kg/cm ³
Young's modulus	235,000 MPa	200,000 MPa
Poisson's ratio	0.3	0.3
Tensile yield strength	3920 MPa	250 MPa
Tensile ultimate strength	3920 MPa	460 MPa

Table 3. Physical characteristics of wind turbine [5]

Property	65-kW Turbine	1-MW Turbine
Hub diameter, length	0.4, 0.25 m	1.6, 0.5 m
Hub height	22.6 m	61.14 m
Rotor blades diameter	16 m	60.62 m
Rotor blades mass	6400 kg	42,000 kg
Rotor blades thickness	60 mm	480 mm
Nacelle width, height, length	1.45, 1.4, 3.28 m	3.93, 3.93, 10.09 m
Nacelle mass	2400 kg	53,700 kg
Tower diameter outer, bottom	2.02 m	3.875 m
Tower diameter outer, top	1.06 m	2.45 m
Tower length	21.9 m	57.19 m
Tower mass	1900 kg	78,600 kg
Tower thickness	5.3 mm	18 mm

Table 4. Dimensions of soil and foundation of the structure [5]

Part	65-kW Turbine	1-MW Turbine
Spread footing pedestal height	0.253 m	0.658 m
Spread footing pedestal diameter	2.314 m	6.016 m
Spread footing center height	0.758 m	1.971 m
Spread footing outer height	0.673 m	1.75 m
Spread footing diameter	7.576 m	19.698 m
Soil depth	8 m	10 m
Soil widths	15 & 22.5 m	38 & 38 m

**Figure 1. Blade dimensions**

3. Numerical models of soil

To study the effects of the soil-foundation-structure interaction, the soil effect can be implicit or explicit. In implicit methods, soil effects are added to the investigation utilizing springs and dampers without modelling the soil. Different implicit analysis techniques use

various assumptions which are proper for specific problems. In an explicit method, the soil is modelled with finite elements. The soil body must be large sufficiently to be precise and, therefore, leads to more time-consuming compared to the implicit method. The implicit method is usually utilized in critical problems.

Two standard implicit methods are: linear soil pressure distribution and the K-model.

3-1- Linear soil pressure distribution model

In this approach, the pressure of soil is supposed to be distributed linearly beneath the foundation. This soil pressure depends solely on the foundation forces and nonlinear reactions cannot be modeled. The linear direct pressure distribution model is a reasonable approximation for rigid foundations such as column foundations.

3-2- K-Model

This implicit method simulates the behaviour of the soil by a sequence of elastic springs beneath the foundation and results in a nonlinear soil pressure distribution

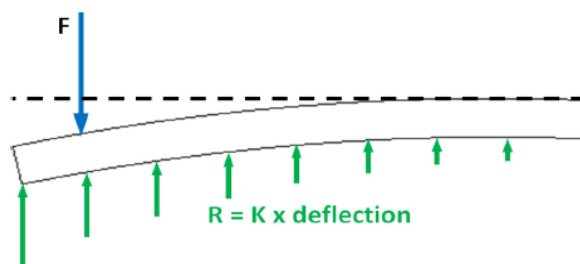


Figure 2. Soil pressure distribution in model K [5]

4. Model Validation

In this section, the validity of the results obtained from modelling two 65-kW and 1-MW wind turbines where springs have replaced soil has been used to compare the frequency outputs with the paper by Austin et al [5]. According to the Iranian instruction for seismic rehabilitation of existing buildings

proportional to the foundation settlement. The spring stiffness of the K-model is referred to as K or modulus of subgrade reaction. The K-model is commonly employed to investigate foundations beneath single concentrated load. In the K-model, K is a combination of structure stiffness and soil and, therefore, it must be determined by trial and error in the design situation. Fig. 2 depicts the soil pressure distribution in the K-model.

In the implicit method, the set of system equations is solved directly, for this reason, the time analysis of the implicit method will be more compared to the explicit method. In contrast, the accuracy of the results of the implicit method in adapting to reality will be better than the explicit method. In this paper, the implicit method has been used to verify the k-model.

(code No. 360) for spring design and calculation of spring stiffness, if the foundation under study is rigid, springs can be used in modeling in the direction of the degree of freedom, and the stiffness coefficients of these springs are obtained according to the following relations.

$$K_x = \frac{G_{max} B}{2 - \nu} \left[3.4 \left(\frac{L}{B} \right)^{0.65} + 1.2 \right] \quad (1)$$

$$K_y = \frac{G_{max} B}{2 - \nu} \left[3.4 \left(\frac{L}{B} \right)^{0.65} + 0.4 \frac{L}{B} + 0.8 \right] \quad (2)$$

$$K_z = \frac{G_{max} B}{1 - \nu} \left[1.55 \left(\frac{L}{B} \right)^{0.75} + 0.8 \right] \quad (3)$$

Where K is the stiffness coefficients of springs, B is the width the foundation, L is length of the foundation, and G_{\max} is dynamic

shear modulus. According to the Spread footing diameter from Table 4, the value of B is equal to:

Table 5. Structural foundation dimensions

65-kW Turbine	1-MW Turbine
$B=7.576\text{m}$	$B=19.698\text{m}$

According to the above formulas, the k values for a wind turbine are presented in Table 6. The results obtained from the paper by Austin et al. [5] are presented in Table 7. The output frequency in this research is compared with the model of the above paper, in three initial states. These results are presented in Table 8.

As can be seen, the outputs are slightly different from the values expressed in the paper, which could be due to various reasons. As mentioned earlier, there are different methods for soil modelling. In this study, ABAQUS software was used, which could cause minor differences in the results.

Table 6. Stiffness coefficients of springs under wind turbine foundations

	65-kW Turbine	1-MW Turbine
K_x	1.22404×10^{23}	3.18257×10^8
K_y	1.22404×10^{23}	3.18257×10^8
K_z	1.40698×10^{23}	3.65823×10^8

Table 7. Natural frequency in the base paper

Foundation Type	Mode	Frequency (Hz)			
		65-kW Turbine		1-MW Turbine	
		K-Model	Explicit	K-Model	Explicit
Spread	1	1.55	1.55	0.42	0.42
	2	1.59	1.59	0.42	0.42
	3	7.96	3.74	3.10	3.10

Table 8. Natural frequency output of the model

Foundation Type	Mode	Frequency (Hz)	
		65- kW Turbine	1- MW Turbine
Spread	1	1.3976	0.442406
	2	1.4236	0.43033
	3	4.1312	1.6018
	4	5.3368	2.2834
	5	5.5984	2.3984
	6	7.4481	3.4761
	7	7.8865	3.8351
	8	8.2869	3.9494
	9	20.935	8.6267
	10	25.437	9.1659

5. Model analysis with Firuz-Bahram soil

In this section, to confirm the results obtained in the model designed with Firuz-Bahram soil, settlement changes based on modelled soil length and element size are briefly examined. The appropriate selection of element size in numerical analysis plays a key role in achieving greater accuracy of results. The use of small elements, in addition to the need for high-performance computer systems, significantly increases the analysis time. On the other hand, selecting elements with large dimensions also reduces the accuracy of the analysis. For this reason, at least in areas of the model where there is a noticeable change in stiffness (such as the vicinity of structural elements), it is necessary to choose element dimensions as small as possible. In practice, these features are also considered in static analyses, but in dynamic analyses, in addition to the above aspects, the dimensions of the elements must be chosen in such a way that the waves can pass through the elements and not be filtered, so to speak. In this regard, the frequency of the incoming waves and the characteristics of the wave velocity in the environment will play a decisive role.

One of the most important approaches that lead to the absorption of wave energy at the model boundaries is the use of viscous or energy-absorbing boundaries. In the case of earthquakes, seismologists' comment that the relationship between the "depth of the earthquake within the Earth" and the "energy released by the earthquake on the Earth's surface" is that the greater the depth of the earthquake, the less energy reaches the Earth's surface in the same seismic area, and as a result, the risk of its occurrence and the damage caused is reduced. The depth of most earthquakes in Iran is not very deep, and most of the important and destructive earthquakes in Iran have occurred at depths between 8 and 20 kilometers. In this section, the earthquake depth of the 65-kW and 1-MW turbines is considered to be 8 meters and 10 meters, respectively. By examining the meshing shown in Figure 3 and the output of the analysis results based on the size of the soil elements under the turbine foundation as well as the modelled soil length shown in Figures 4 to 5, the following results can be achieved.

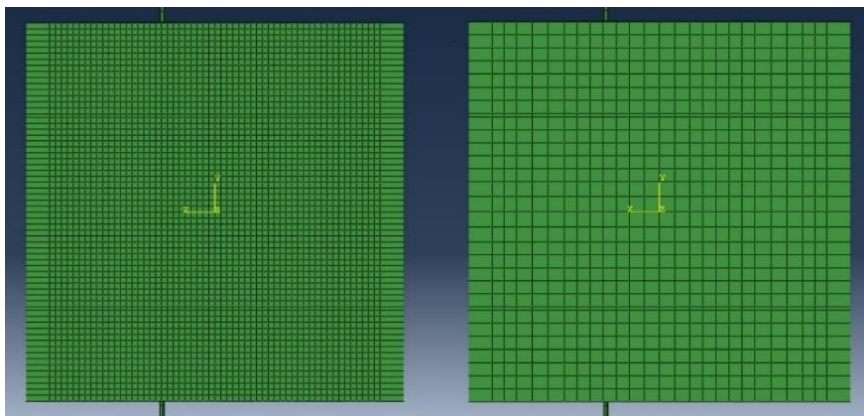


Figure 3. Coarse and fine meshing of the soil beneath the foundation

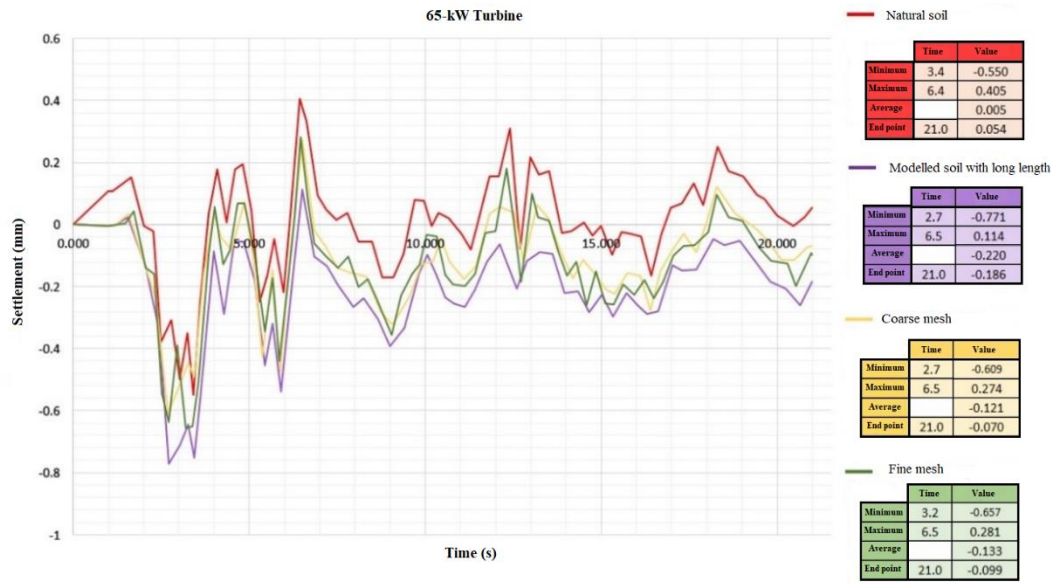


Figure 4. Comparison chart of settlement rates resulting from fine and coarse soil meshing

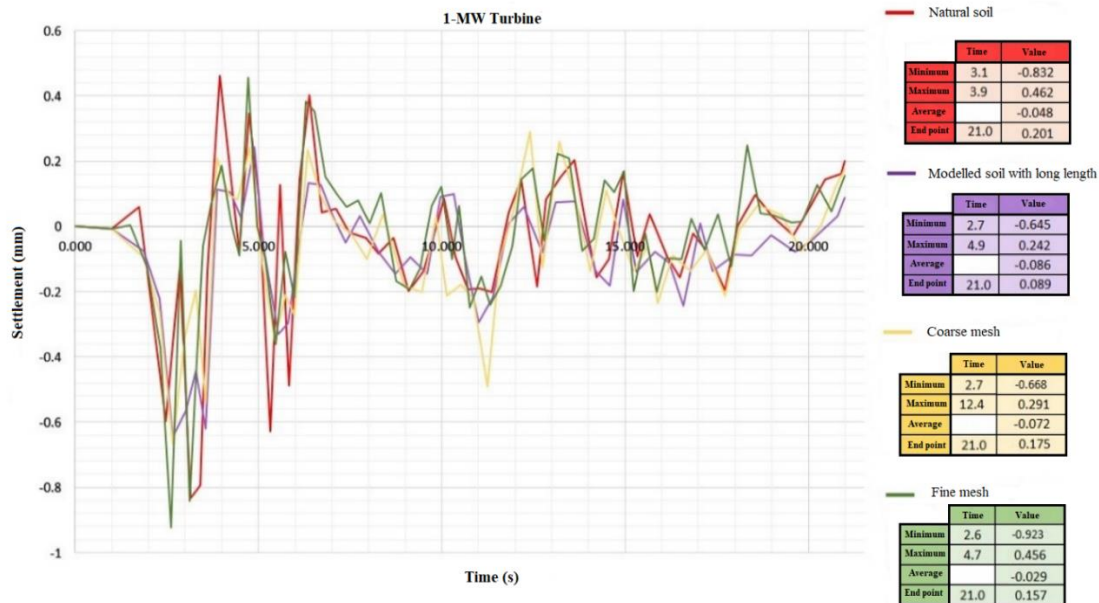


Figure 5. Comparison chart of settlement rates resulting from fine and coarse soil meshing

According to Figures 4 and 5, the settlement change trend for 65-kW and 1-MW turbines modelled with Firuz-Bahram soil with fine and coarse meshing is acceptably similar. The difference in a settlement between modelling with coarse and fine meshing at the endpoint (time 21 seconds) is 0.029 mm for the 65-kW turbine and 0.018 mm for the 1-MW turbine.

6. Method of calculating soil dynamic parameters

In this section, soil information of the study area is presented according to Table 9.

Also, the difference in the average settlement between the modelling with coarse and fine meshing for 65-kW and 1-MW turbines is 0.012 and 0.043 mm, respectively. Due to the low settlement difference of the above four samples, the modelling results were obtained with good accuracy.

According to the information in Table 9, Young's modulus, shear wave velocity, and

dynamic Poisson's ratio were calculated according to the following relationships. Dynamic Young's modulus is also obtained from the following equation:

$$E_i = 2G_{max}(1 + \nu) = 238400 \text{ KN/m}^2 \quad (4)$$

The following equation is used to calculate the shear wave velocity (V_s):

$$G_o = \frac{\gamma \times V_s^2}{g} \Rightarrow V_s = 202.667 \text{ m/s}^2 \quad (5)$$

And also, the following equation is used to calculate Poisson's ratio (ν):

$$\gamma = 3.2V_p^{0.25} \Rightarrow V_p = 1271 \text{ m/s} \quad (6)$$

$$\nu = \frac{\left(\frac{V_p}{V_s}\right)^2 - 2}{2\left(\left(\frac{V_p}{V_s}\right)^2 - 1\right)} = 0.49 \quad (7)$$

Where V_p is pressure wave velocity. Now, in this research, cement has been used as a stabilizing agent. As a result, the effect of 3%, 6% and 8% cement in the soil has been investigated. The values and properties of the amended soil have been presented according to Tables 10 to 12.

Table 9. Soil characteristics of Firuz Bahram

Internal Friction Angle (ϕ)	$^{\circ}7.5$
Coefficient of Adhesion (C)	0.74 Kg/cm^2
Specific Gravity (γ)	19.107 KN/m^3
Dry Specific Gravity (γ_d)	16.5 KN/m^3
Moisture Percentage (w)	15.8%
Young's Modulus	36250 KN/m^2
Poisson's Ratio (ν)	0.49
Plastic Index ($P.I$)	10%
Uniformity Coefficient (C_u)	25
Dynamic Young's Modulus (E_i)	238400 KN/m^2
Static Shear Modulus (G_o)	12500 KN/m^2
Dynamic Shear Modulus (G_{max})	80000 KN/m^2
Soil Density (ρ)	1.947 KN/m^2

Table 10. Characteristics of Firuz-Bahram soil with the addition of 3% cement

$G=7985924 \text{ Kg/m}^2$	$\phi = 7.6^{\circ}$
	$C=0.76 \text{ Kg/cm}^2$
	$E=23798054 \text{ Kg/m}^2$
	$\gamma=1.90734 \text{ gr/cm}^3$

Table 11. Characteristics of Firuz-Bahram soil with the addition of 6% cement

$G=8314264 \text{ Kg/m}^2$	$\phi = 8.8^{\circ}$
	$C=1.09 \text{ Kg/cm}^2$
	$E=24776508 \text{ Kg/m}^2$
	$\gamma=1.94712 \text{ gr/cm}^3$

Table 12. Characteristics of Firuz-Bahram soil with the addition of 8% cement

$G=8166633 \text{ Kg/m}^2$	$\phi = 10.7^{\circ}$
	$C=1.61 \text{ Kg/cm}^2$
	$E=24336565 \text{ Kg/m}^2$
	$\gamma=1.9505 \text{ gr/cm}^3$

7. Earthquake record

After modelling in ABAQUS software, the acceleration data of the 1940 El Centro earthquake was used for seismic analysis of

the structure, and its seismic response diagram is presented (Figure 6) according to the book Structural Dynamics [22].

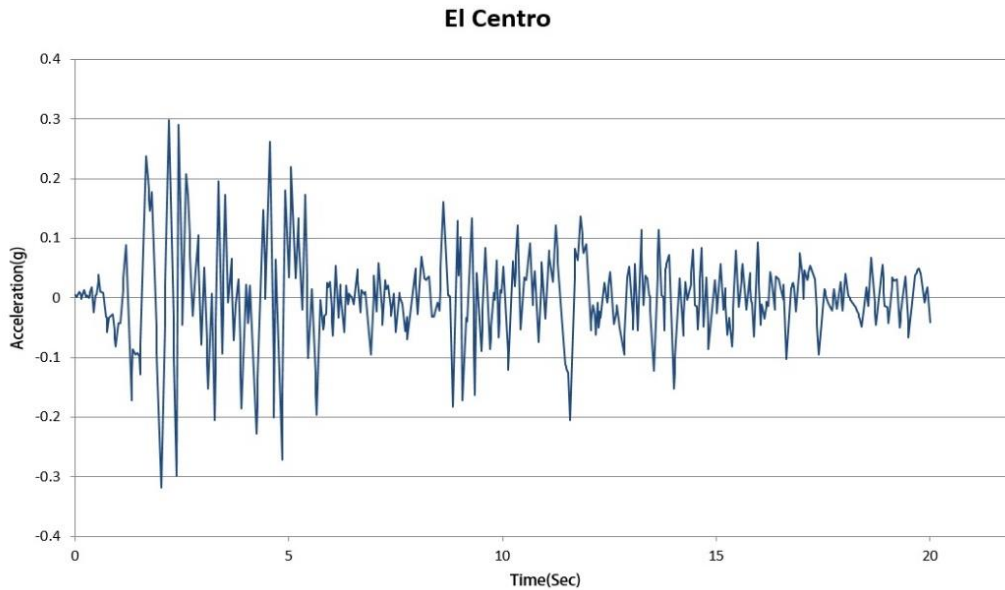


Figure 6. Seismic records of the El Centro earthquake

8. Displacement study

In accordance with the research objectives, points for vertical and horizontal displacement were considered and the changes in these points were examined within 20 seconds. The characteristics and extent of changes in these points are shown in Figure 7.

8-1- Vertical displacement

The vertical displacement was investigated at three points, including the centre under the foundation and two other points at the edge of the foundation. The amount of these changes was measured over a period of 20 seconds, and from the results obtained, it can be seen that in this period of time and natural soil, the displacement for the 65-kW turbine has the highest settlement at $t=20s$, which is equal to 0.35 mm. In the next step, these changes were compared at the same point with the modified soil, so that the changes in vertical displacement in the 65-kW turbine at the central point with the soil stabilized with 3% cement were very insignificant, and these changes decreased slightly, which is

equivalent to 0.317 mm. Further, to observe other changes, stabilization with 6 and 8 percent cement was also investigated. As can be seen in the graph in Figure 8, the amount of settlement for soil stabilized with these amounts of cement continues to decrease.

The variations of the 1-MW turbine are also presented in Figure 9. As can be seen, the settlement rate increased by 47.4% for the soil stabilized with 3% cement and then an increasing trend was observed at a higher stabilization percentage, i.e. 6% cement, but this rate reached its lowest value, i.e. 19 mm in the soil stabilized with 8%.

The vertical displacement at the front corner of the foundation is the second point for investigating settlement changes. The output of the changes for the 65-kW turbine is shown in Figure 10. As can be seen, the settlement of the Firuz-Bahram soil at this point is 0.691 mm. The effect of soil stabilized with cement has reduced the settlement by 0.08 mm. The trend of settlement changes at higher cement percentages has decreased significantly. In the larger turbine, the settlement in the Firuz-Bahram soil is 0.836 mm, which is a decrease

from the settlement in the soil stabilized with 3% and 6% cement.

Also, the settlement in the soil stabilized with 6% cement has experienced a 40.43% decrease compared to Firuz-Bahram soil. However, in the soil stabilized with 8% cement, it has increased by 43.59% compared to soil stabilized with 6% cement. The overall changes for the 1-MW turbine are presented in Figure 11.

The changes at the last point, which is at the back corner beneath the foundation, according to the outputs of the 65-kW turbine, are 0.857 mm for the Firuz-Bahram soil. This settlement amount has decreased by 0.135

mm compared to the soil stabilized with 3% cement. Also, in soil stabilized with 6% cement, settlement initially decreased by 0.207 mm, and then this amount decreased by 0.542 mm in soil stabilized with 8% cement compared to Firuz-Bahram soil. The relevant changes can be seen in the graph of Figure 12. For the 1-MW turbine, the settlement amount in the soil stabilized with 3% cement has declined slightly compared to the Firuz-Bahram soil, this decreasing trend is also observed in the 6% cement. Eventually, at higher percentages, the settlement trended upward again. For a more detailed view of the changes, see Figure 13.

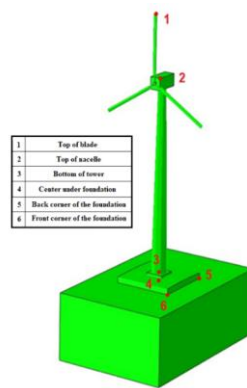


Figure 7. Location of points examined for vertical displacement

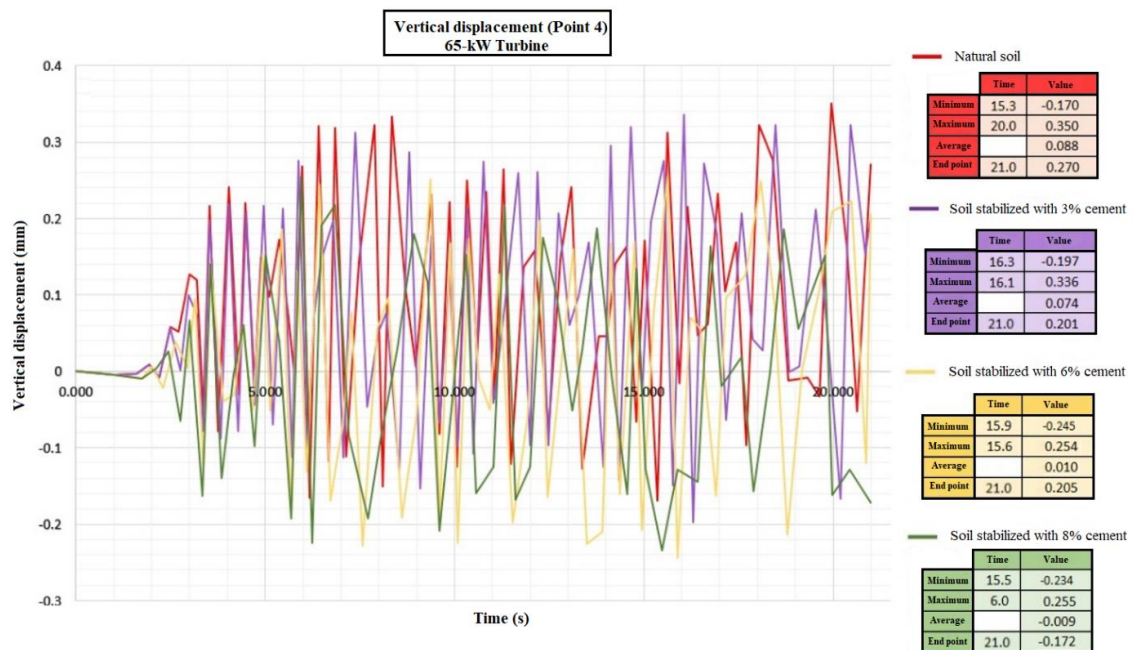


Figure 8. Vertical displacement of 65-kW turbine with different cement percentages

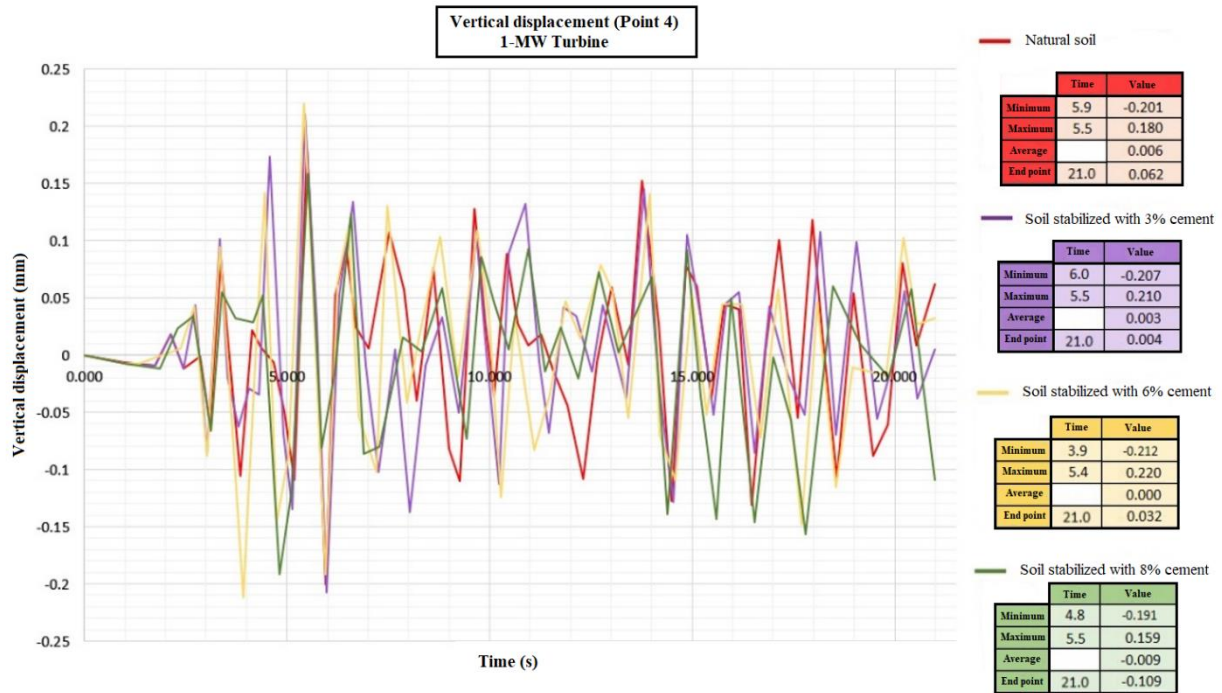


Figure 9. Vertical displacement of 1-MW turbine with different cement percentages

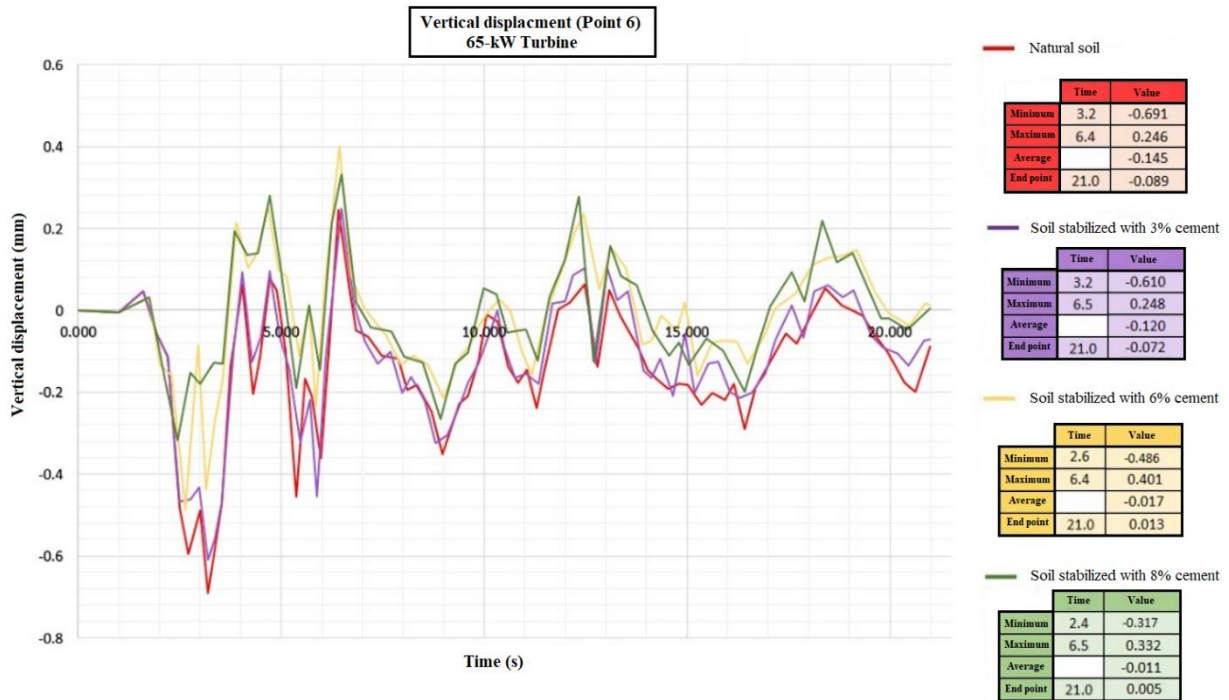


Figure 10. Vertical displacement of 65-kW turbine with different percentages of cement at the corner of the foundation

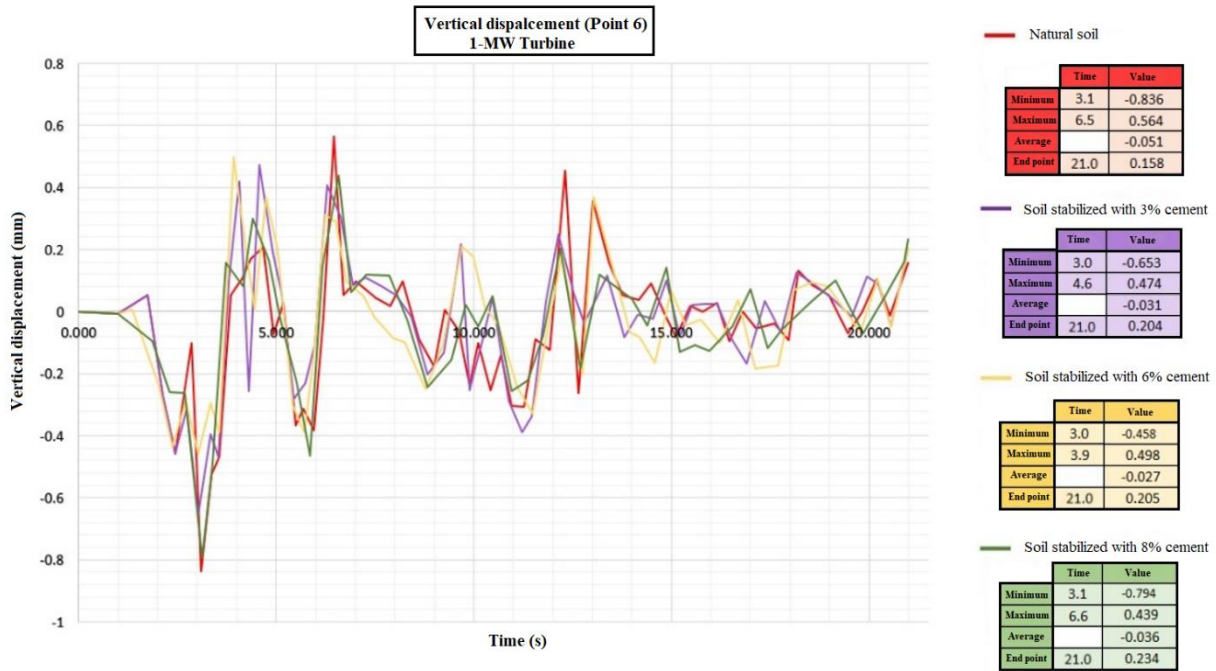


Figure 11. Vertical displacement of 1-MW turbine with different percentages of cement

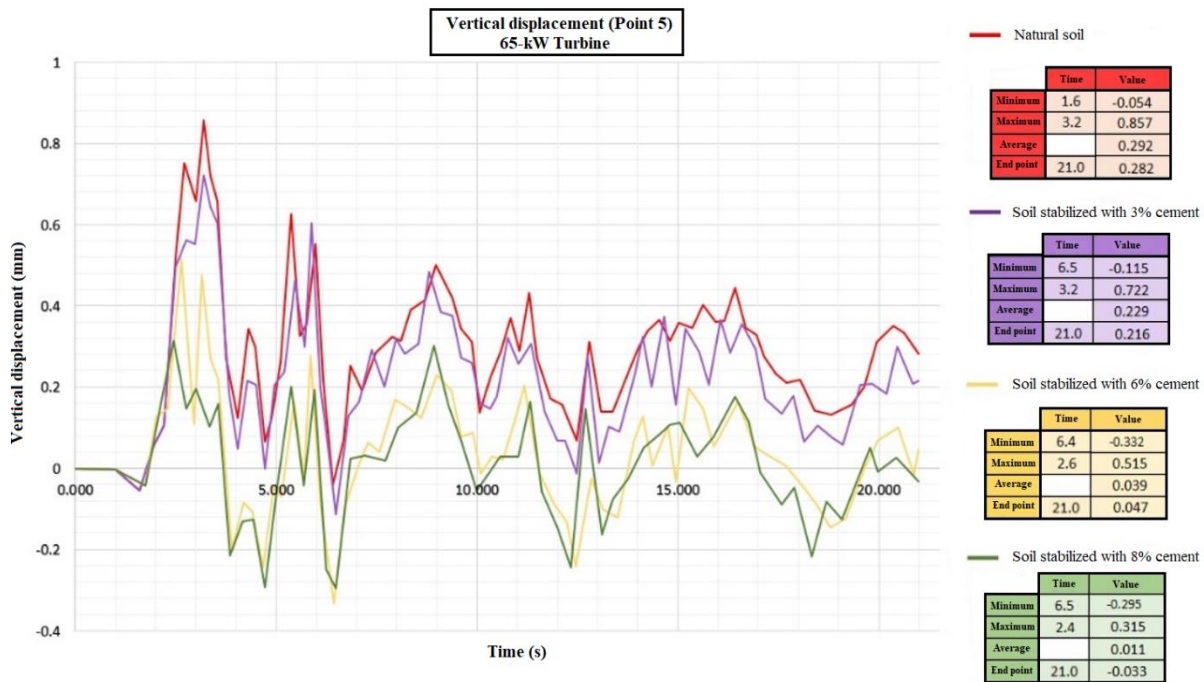


Figure 12. Vertical displacement of 65-kW turbine with different percentages of cement in the back corner

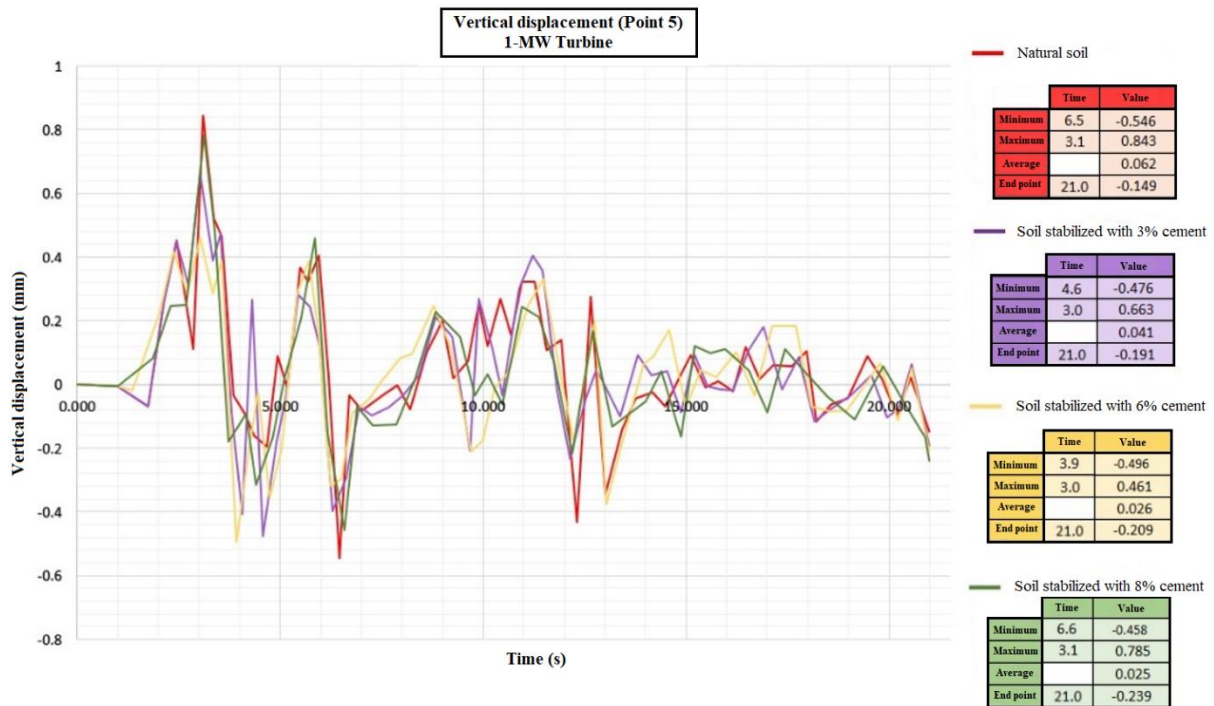


Figure 13. Vertical displacement of 1-MW turbine with different percentages of cement in the back corner

8-2- Horizontal Displacement

In this section, the difference in horizontal displacement at three points above the blade, the nacelle, and a point on the foundation relative to a point in the center of the soil is reported. Figure 14 shows the results obtained from this difference in displacement at the top of the blade of a 65-kW turbine. As can be seen, the displacement in the soil stabilized with 3% cement has increased by 0.73 mm compared to the Firuz-Bahram soil. These values for higher cement percentages first increased by 0.42 mm in soil stabilized with 6% cement, then with the addition of more cement, the horizontal displacement in soil stabilized with 8% cement reached its lowest value, so that it decreased by 6.8 mm compared to the Firuz-Bahram soil.

In the 1-MW turbine, as shown in Figure 15, the results obtained indicate a difference in displacement at the top of the blade of this turbine. As can be seen, the displacement in the soil stabilized with 3% cement has decreased by 11.49 mm compared to the Firuz-Bahram soil. In the soil stabilized with 6% cement, the horizontal displacement

increased by 8.86 mm compared to the soil stabilized with 3% cement. Finally, by adding 8% cement, the horizontal displacement in the soil stabilized with 8% cement decreased by 3.24 mm compared to the soil stabilized with 6% cement.

The difference in horizontal displacement at the top of the nacelle relative to the point at the center of the soil is reported. Figure 16 shows the results of this difference in displacement at the top of the nacelle of the 65-kW turbine. As can be seen, the displacement value in the soil stabilized with 3% cement has increased by 3.47 mm compared to the Firouz Bahram-soil. These values have a decreasing trend for higher percentages of cement. Reaching its lowest value in the soil stabilized with 8% cement, the horizontal displacement in the soil stabilized with 8% cement has decreased by 6.94 mm compared to the Firuz-Bahram soil.

In the 1-MW turbine, as shown in Figure 17, the results show the difference in displacement at the top of the turbine nacelle. As can be seen, the displacement in the soil stabilized with 3% cement has decreased by 0.95 mm compared to the Firuz-Bahram soil.

However, in the 6% stabilized soil, the horizontal displacement increases, which increases by 0.31 mm compared to the soil stabilized with 3% cement. Finally, the addition of 8% cement has created the lowest horizontal displacement, which has significantly decreased by 13.14 mm compared to the Firuz-Bahram soil. Finally, the difference in horizontal displacement at the front corner of the foundation relative to the point in the center of the soil is reported. Figure 18 shows the results of this difference in displacement for the 65-kW turbine. As can be seen, the displacement in the soil stabilized with 3% cement increased by 0.03 mm compared to the Firuz-Bahram soil. These

values decreased slightly for higher cement percentages. The horizontal displacement in the soil stabilized with 8% cement decreased by 0.01 mm compared to the Firouz-Bahram soil. In the 1-MW turbine, the results obtained show the difference in displacement in this turbine (see Figure 19). As can be seen, the displacement in the soil stabilized with 3% cement decreased by 0.11 mm compared to the Firuz-Bahram soil. It can be seen that the difference in horizontal displacement increases slightly with the addition of higher amounts of cement. The horizontal displacement in the soil stabilized with 8% cement also increased very slightly by 0.07 mm compared to 6% cement.

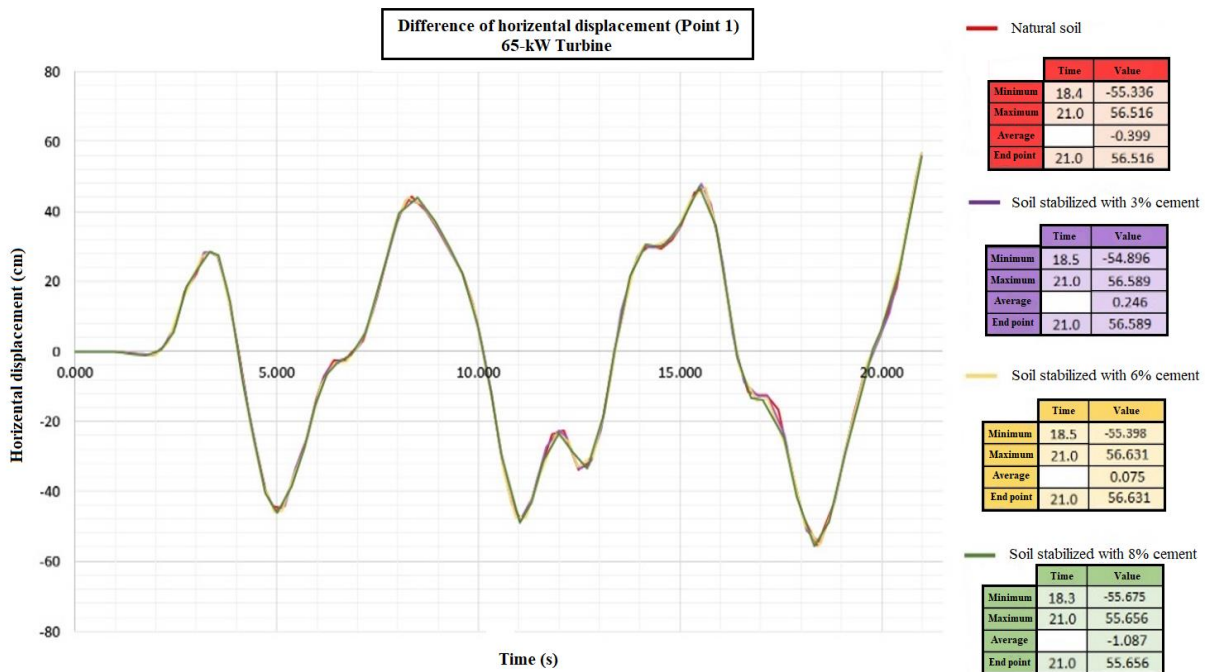


Figure 14. Horizontal displacement of a 65-kW turbine at the top of the blade.

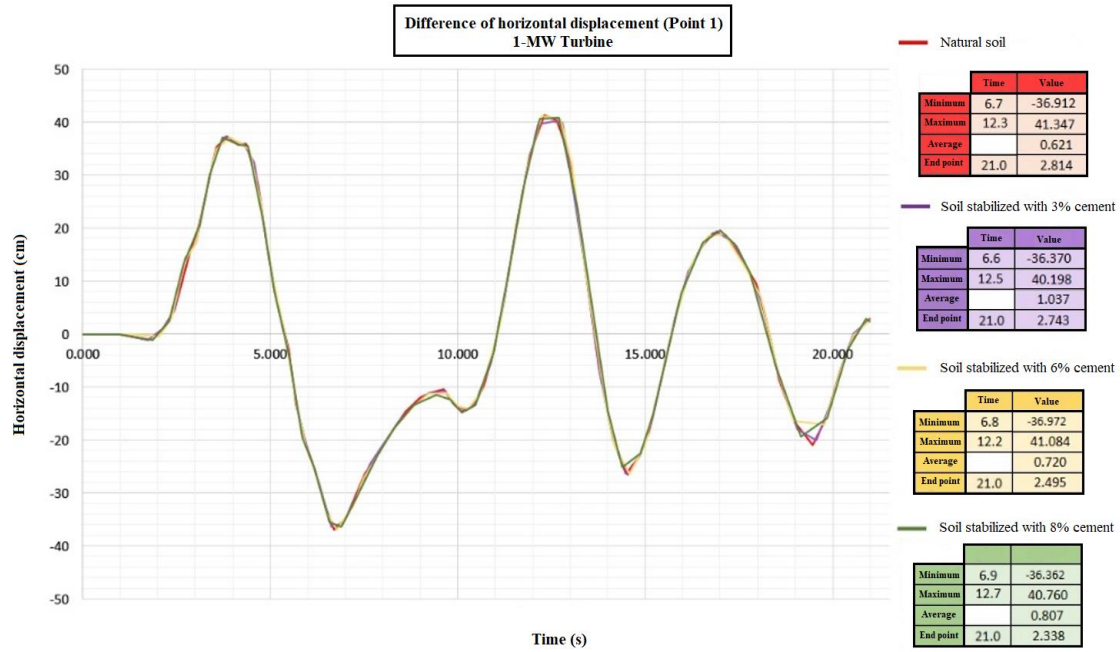


Figure 15. Horizontal displacement of a 1-MW turbine at the top of the blade.

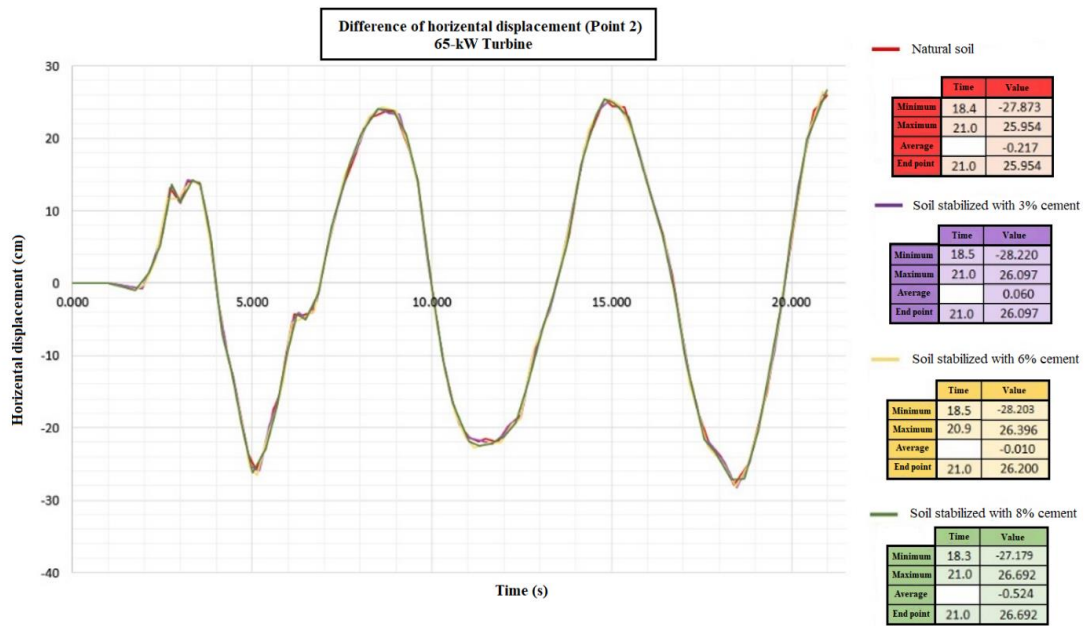


Figure 16. Horizontal displacement of a 65-kW turbine at the top of the engine (nacelle)

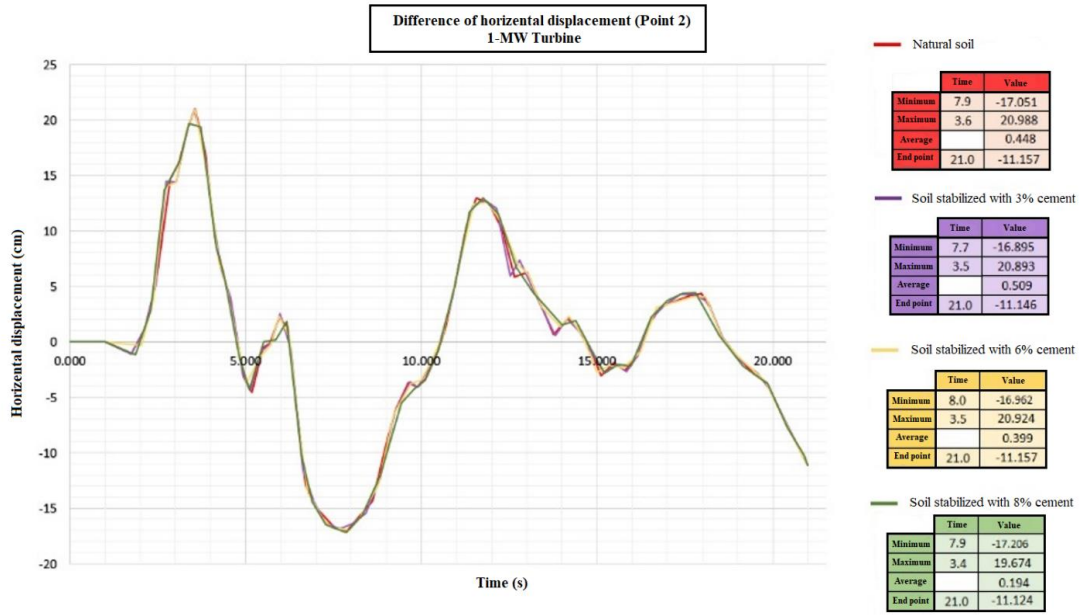


Figure 17. Horizontal displacement of a 1-MW turbine at the top of the engine (nacelle)

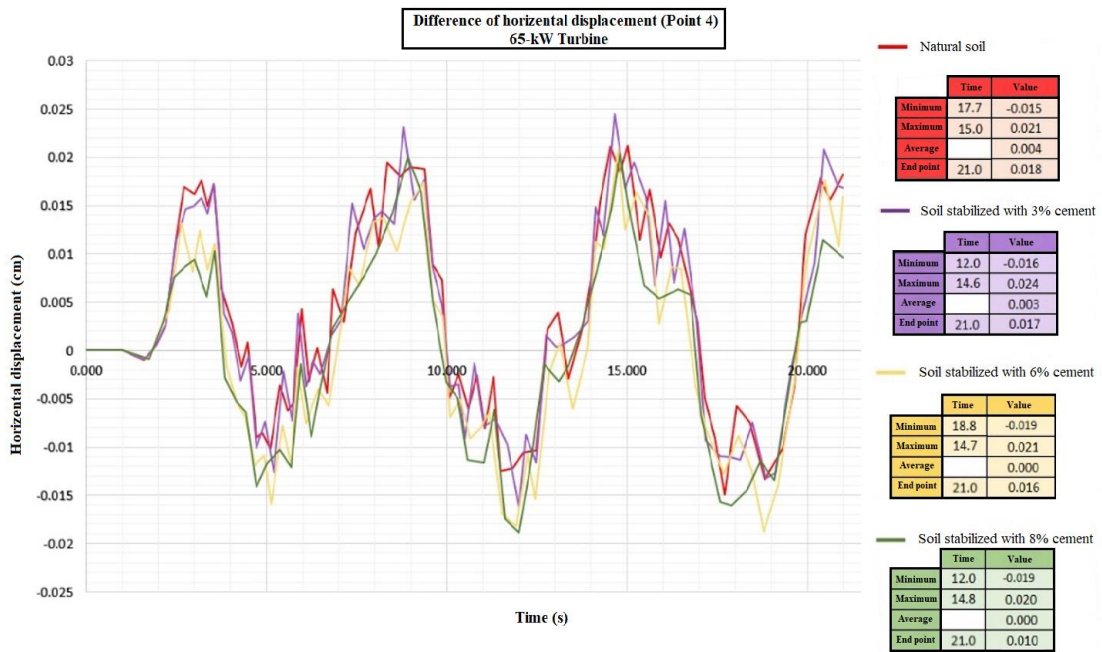


Figure 18. Horizontal displacement of a 65-kW turbine at the center point of the sub-base

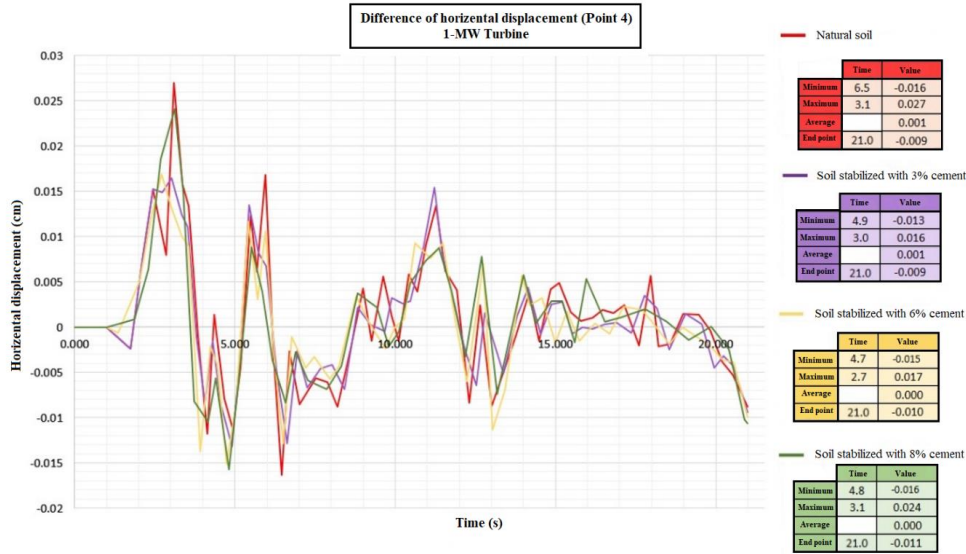


Figure 19. Horizontal displacement of a 1-MW turbine at the center point of the sub-base

8-3- Base Shear force

In the final step, the base shear force in a 65-kW wind turbine was investigated in a 20-second time interval in Firuz-Bahram soil as shown in Figure 20. The base shear force was extracted from the bottom point of the vertical tower rod. In natural soil, the base shear force has reached a maximum value of 29.948 KN. In soil stabilized with different percentages of cement, the trend of base shear force is increasing. For soil stabilized with 3% cement, it increased by 3.525 KN, 6% decreased by 0.274 KN compared to the lower percentage of the additive, and finally,

in soil stabilized with 8% cement, it decreased by 0.477 KN compared to 6% cement. In a 1-MW turbine, as shown in Figure 21, the results obtained indicate the base shear force in this turbine.

As can be seen, the base shear force in the soil stabilized with 3% cement decreased by 0.969 KN compared to Firuz-Bahram soil, increased by 0.608 KN for soil stabilized with 6% cement compared to soil stabilized with 3% cement, and finally reached its lowest value of 18.453 KN in soil stabilized with 8% cement, which has decreased by 457.5 KN compared to Firuz-Bahram soil.

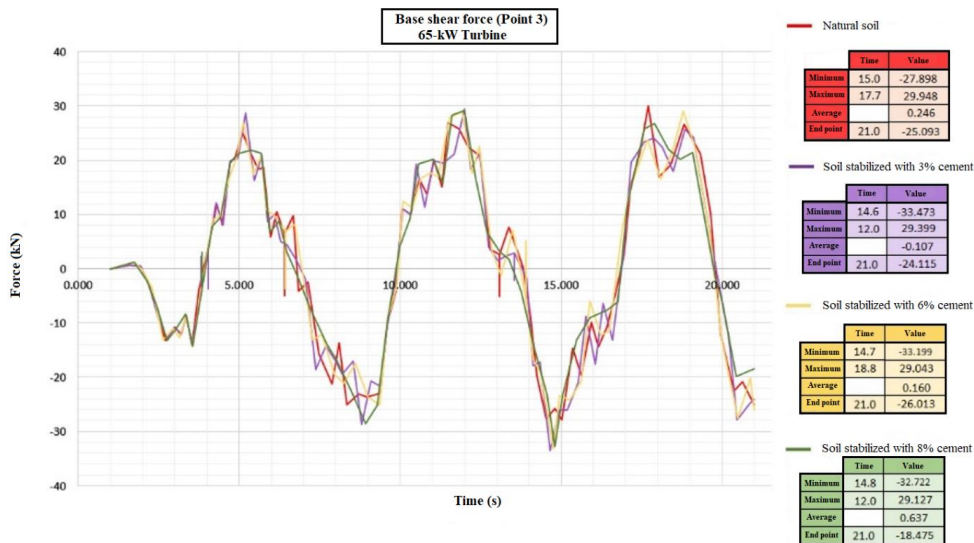


Figure 20. 65-kW turbine base section at tower bottom point

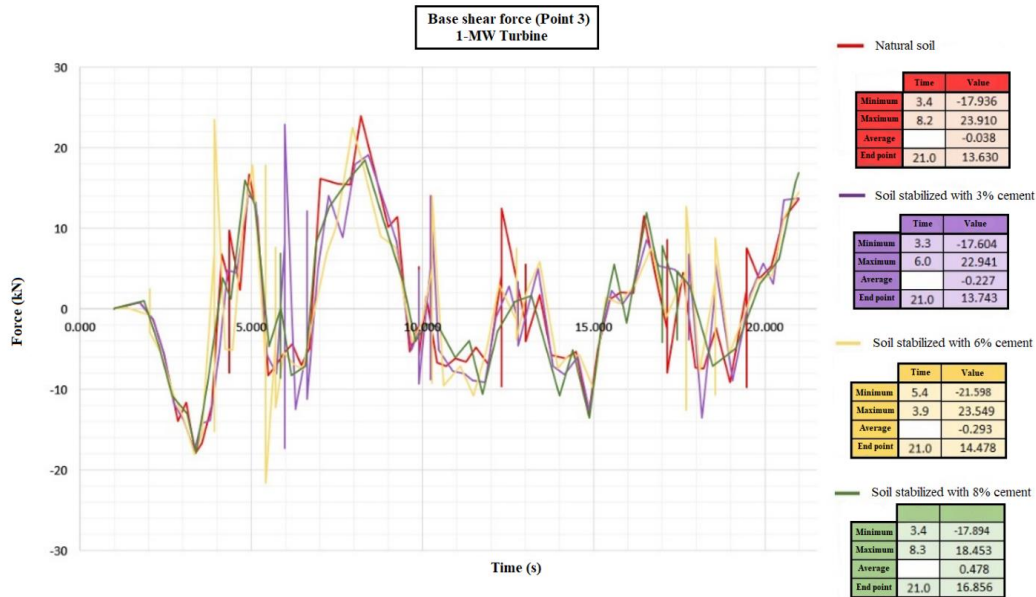


Figure 21. 1-MW turbine base section at tower bottom point

8-4- Investigation of stress changes

To compare the stress changes in the two natural and stabilized soils, the soil stress contour along both soils has been investigated. Next, the maximum stress contour values for the 65-kW turbine will be investigated. As can be seen in Figure 22, the maximum stress for the Firuz-Bahram soil at $t=14.02s$ is 6.702×10^4 Pascal. In the soil stabilized with 3% cement, the maximum values at $t=13.65$ are 9.105×10^4 Pascal. In the soil stabilized with 6% cement, the maximum values at $t=13.74$ are 8.576×10^4 Pascal and finally in the soil stabilized with 8% cement, the maximum stress values at

$t=13.81$ are 8.325×10^4 Pascal. The overall stress contour changes are presented in Figures 23, 24 and 25. The maximum stress contour for a 1-MW turbine is shown in Figure 29. As can be seen in Figure 26, the maximum stress for the Firuz-Bahram soil at $t=13.84s$ is 8.831×10^3 Pascal. In the soil stabilized with 3% cement, the maximum values at $t=4.977s$ are 1.754×10^4 Pascal. In the soil stabilized with 6% cement, the maximum values at $t=4.7s$ are 2.134×10^4 Pascal, and finally, in the soil stabilized with 8% cement, the maximum stress values at $t=9.46s$ are 1.141×10^4 Pascal. The overall changes in the stress contour are presented in Figures 27, 28, and 29.

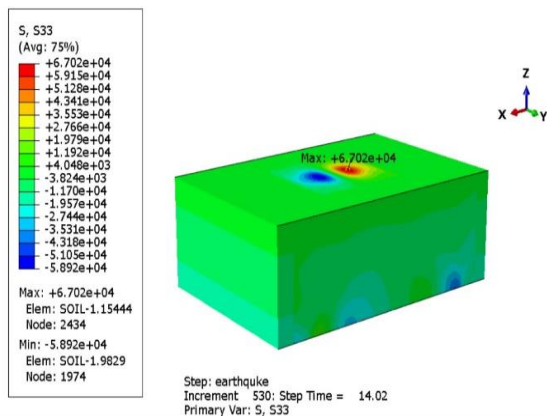


Figure 22. Stress contour of 65-kW turbine in Firuz-Bahram soil

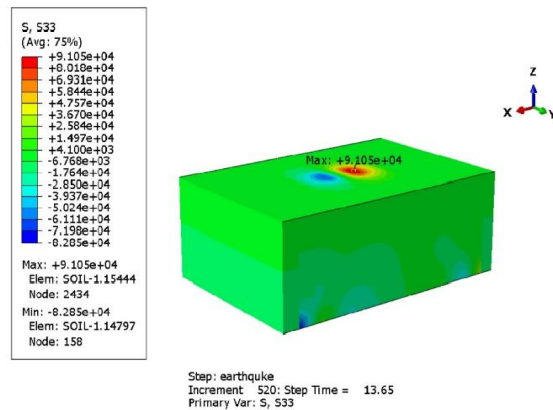


Figure 23. Stress contour of 65-kW turbine in amended with 3% cement

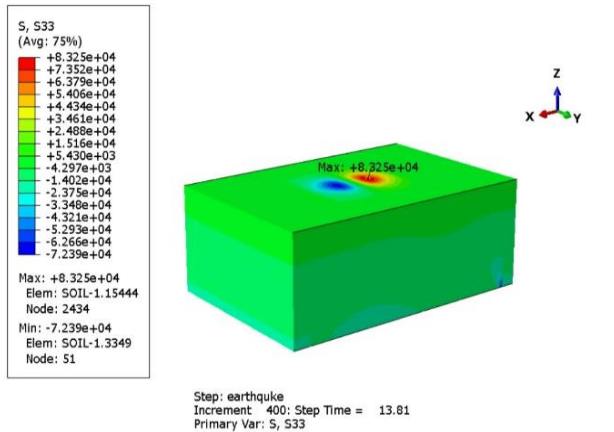


Figure 24. Stress contour of 65-kW turbine in amended with 8% cement

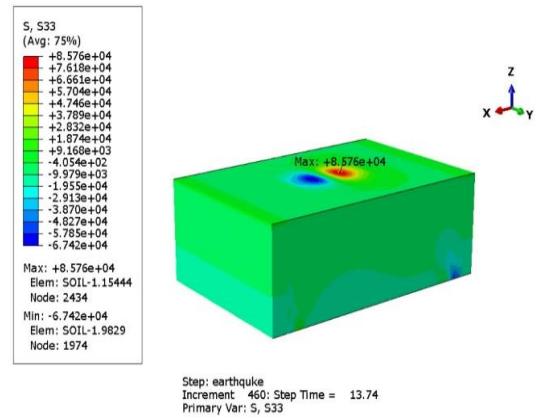


Figure 25. Stress contour of 65-kW turbine in amended with 6% cement

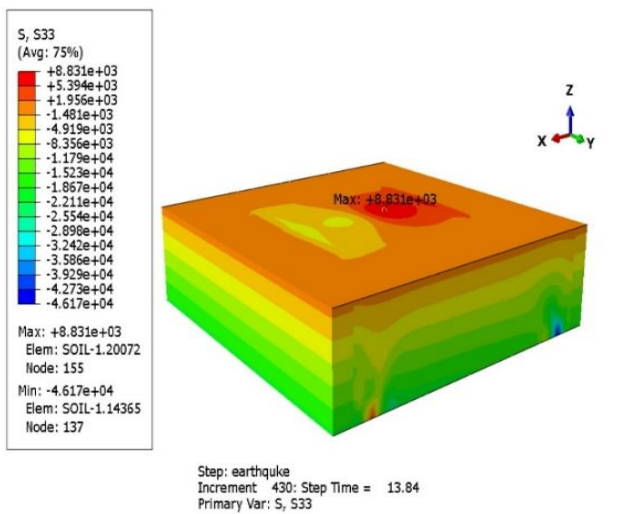


Figure 26. Stress contour of 1-MW turbine in Firuz-Bahram soil

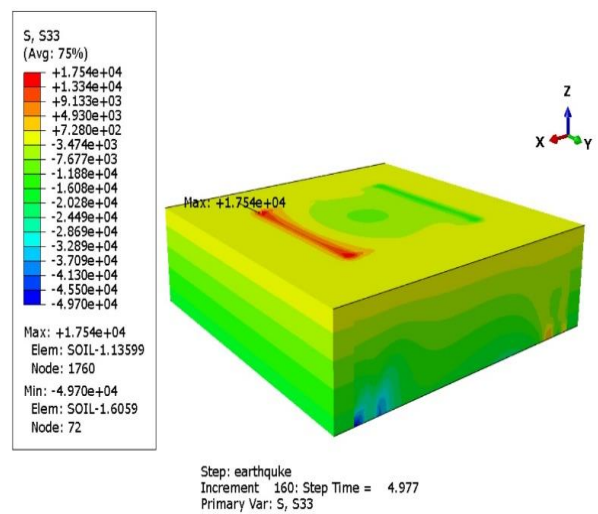


Figure 27. Stress contour in soil amended with 3% cement

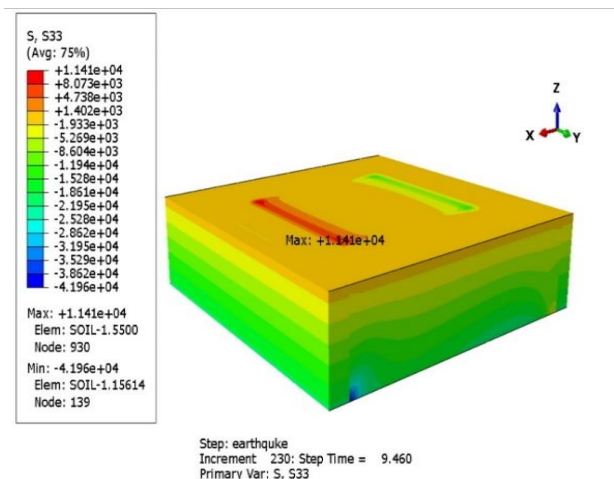


Figure 28. Stress contour in soil amended with 6% cement

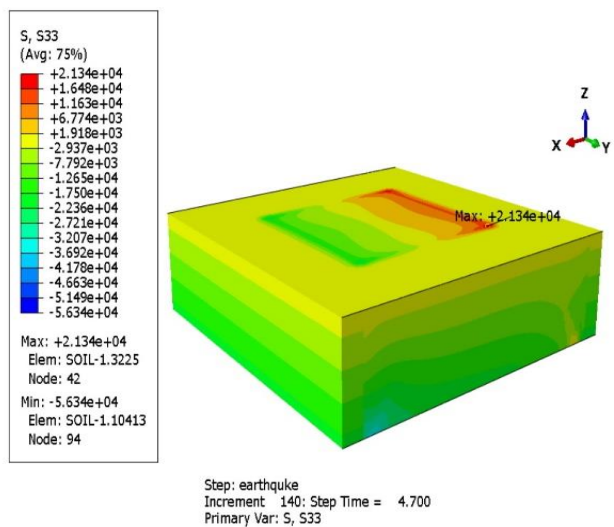


Figure 29. Stress contour in soil amended with 8% cement

8-5- Output frequency

This section examines the output frequency of 65-kW and 1-MW turbines. The natural frequencies in Firuz-Bahram soil in 5 cases

have been extracted from the software for comparison with soil modified with different percentages of cement. The results obtained for both turbines are presented in the following tables (see Table 13):

Table 13. Output frequency of two turbines in all three soil models

Soil	Mode No	Frequency (Hz)	
		65- kW Turbine	1- MW Turbine
Firuz-Bahram	1	0.16572	0.06219
	2	0.16961	0.06399
	3	0.40335	0.15606
	4	0.54021	0.23651
	5	0.57432	0.24750
Soil stabilization with 3% cement	1	0.16569	0.06219
	2	0.16958	0.06398
	3	0.40334	0.15606
	4	0.54019	0.23650
	5	0.57429	0.24749
Soil stabilization with 6% cement	1	0.16572	0.06219
	2	0.16960	0.06399
	3	0.40335	0.15606
	4	0.54021	0.23651
	5	0.57432	0.24750
Soil stabilization with 8% cement	1	0.16572	0.06.219
	2	0.16961	0.06399
	3	0.40335	0.15606
	4	0.54021	0.23651
	5	0.57432	0.24750

9. Discussion and analysis of results

In this section, the analysis of the vertical displacement results is first discussed. The changes in the 65-kW turbine decrease with soil stabilization so that by adding 8% cement to the soil, the largest change is observed, equivalent to 0.542 mm, according to Figure 12. However, in the 1-MW turbine, Figure 13, the largest changes will be in the soil stabilized with 6% cement, and at higher percentages, the settlement will increase again. The horizontal displacement of the 65-kW turbine (Figure 14) at the top of the blade for the soil stabilized with 8% cement has the largest decrease of 8.6 mm, but in the 1-MW turbine (Figure 15) the largest change

is in the soil stabilized with 3% cement, which increases by 11.49 mm.

In the horizontal displacement of the 65-kW turbine (Figure 16) above the nacelle, it is observed that soil stabilization initially increased the horizontal displacement, but in the soil stabilized with 8% cement, the horizontal displacement decreased by 6.94 mm. Also, in the 1-MW turbine (Figure 17), the horizontal displacement in the soil stabilized with 3% and 6% cement decreased slightly compared to the Firuz-Bahram soil. Finally, the soil stabilized with 8% cement decreased by 13.14 mm compared to the Firuz-Bahram soil. At the last point, the horizontal displacement on the foundation for the 65-kW turbine (Figure 18), the soil stabilized with cement initially increased

slightly and returned to the initial value with the addition of 6% cement, and there was no change in the horizontal displacement. However, stabilization with 8% cement shows that the displacement will decrease by 0.01 mm compared to the Firuz-Bahram soil. For the 1-MW turbine (Figure 19), at this point, the horizontal displacement initially decreased by 0.11 mm with the addition of 3% cement, and finally, the addition of 6% and 8% cement caused a slight increase in the values compared to the soil stabilized with 3% cement.

From the comparison of the two graphs (20) and (21) for the base shear, it is concluded that the base shear in the smaller turbine with a higher cement percentage has an increasing trend and its highest value is observed in the soil stabilized with 3% cement. In the 1-MW turbine, the Firuz-Bahram soil initially showed a very slight decreasing trend compared to the soil stabilized with 3% cement, but with increasing the amount of cement, the base shear also increased and finally with the addition of 8% the base shear decreased significantly.

In Figures (23), (24) and (25), by comparing the three stress contours in the 65-kW turbine, it is observed that its maximum values have increased significantly in the stabilized soil so that the values first increased significantly in the soil stabilized with 3% cement, and then in the soil stabilized with 6% and 8% cement, these values decreased compared to the soil stabilized with 3% cement. In the 1-MW turbine, from the comparison of Figures (27), (28) and (29), it is concluded that the stress in the soil stabilized with 3% cement has significantly increased compared to the natural soil, and also higher values of the stress contour have been observed in the soil stabilized with 6% cement. However, these changes decrease again in the soil stabilized with 8% cement.

The natural frequencies in both turbines were compared, and in the 65-kW turbine, the output frequency decreased by 3% compared to the soil stabilized with cement, and at higher percentages, the frequency increased slightly. In the 1-MW turbine, these changes

were also very small, and in general, a decreasing and then increasing trend is observed (like the 65-kW turbine).

10. Conclusion

The research results can be classified into two groups. The first group includes the results related to the 3D modelling method of 65-kW and 1-MW wind turbines on Firuz-Bahram soil, considering the effects of soil-foundation-structure interaction. The second group includes the results related to the detailed study of the effects of soil-structure interaction, considering the stabilization of Firuz-Bahram soil with 3%, 6% and 8% cement, as well as considering the seismic effects on the turbine.

The output of the first phase of the study will be of great importance as a tool for extracting the results of the second phase. Therefore, the present study provides a coherent set of steps forward in the direction of wind turbine investigation and investigation in the field of earthquake engineering. The output of the first phase of the study will be of great importance as a tool for extracting the results of the second phase. Therefore, the present study provides a coherent set of steps forward towards the investigation and study of wind turbines in the field of earthquake engineering.

- By considering the effects of soil-structure interaction in wind turbine modelling, the natural frequencies of the tower are reduced.
- Adding cement to the soil reduces soil settlement, which is recommended as the optimal value with 8% and 6% cement for a 65-kW and 1-MW turbine, respectively.
- In 65-kW and 1-MW turbines, adding cement to the soil reduces the horizontal displacement.
- The results of the base shear force analysis in a 65-kW turbine show that the base shear rises with increasing cement content.

- In a 65-kW and 1-MW turbine, adding cement to the soil increases the stress contour.

References

- [1]. M.Massah-Fard, A.Erken, B.Erkmen, A.Ansal, “Analysis of Offshore Wind Turbine by Considering Soil-Pile-Structure Interaction: Effect of Sea-Wave Load Duration, *Journal of Earthquake Engineering*, Pages 3291-3309 | Received 22 Jul 2022, Accepted 27 Mar 2024, Published online: 11 Apr 2024, <https://doi.org/10.1080/13632469.2024.2337848>
- [2]. Ferreira, G.Vernizzi, M.Futai, G.Franzini “Modeling strategies for wind turbines considering soil–structure interaction”, *Ocean Engineering*, Volume 309, Part 1, 1 October 2024, 118310, <https://doi.org/10.1016/j.oceaneng.2024.118310>
- [3]. F.Moghadam-Rad, P.Zarfam, M.Zabihi-Samani, “The effect of dolphin echolocation-fuzzy logic controller in semi-active control of structural systems using endurance time method”, *Scientia Iranica, Sharif University of Technology*, (2024) 31(7), 541-555, DOI: 10.24200/sci.2023.57268.5147
- [4]. Global Wind Energy Council. Global wind report annual market update 2014
- [5]. S.Austin, S.Jerath, “Effect of soil-foundation-structure interaction on the seismic response of wind turbines”, *Ain Shams Engineering Journal*, Volume 8, Issue 3, September 2017, Pages 323-331
- [6]. O.Diaz, L.Suarez, “Seismic Analysis of Wind Turbines”, *Sage Journals*, Volume 30, Issue 2, Published 1 May 2014
- [7]. M.VakilZadeh, M.Shayanfar, M.Zabihi-Samani, M.Ravanshadnia, “COMPETENCY-BASED SELECTION AND ASSIGNMENT FOR PROJECT MANAGER IN IRANIAN RAILWAYS PROJECTS BY GENETIC MULTIGENIC PROGRAMMING”, *Journal Decision making: applications in management and engineering*, Vol. 6, Issue 2, 2023, pp. 808-8027, DOI: <https://doi.org/10.31181/dmame622023727>
- [8]. E. Hau, “Wind turbines: fundamentals, technologies, application, economics.”, Springer Verlag, 2006.
- [9]. G. Lloyd, “Guidelines for the Certification of Wind Turbines.”, Hamburg, Germany, 2010.
- [10]. I. Prowell, “An experimental and numerical study of wind turbine seismic behavior.”, University of California, San Diego, 2011.
- [11]. “Guidelines for Design of Wind Turbines.” Copenhagen, Denmark, 2001.
- [12]. I. Lavassas, G. Nikolaidis, P. Zervas, E. Efthimiou, I. N. Doudoumis, and C. C. Baniotopoulos, “Analysis and design of the prototype of a steel 1-MW wind turbine tower,” *Eng. Struct.*, vol. 25, 2003
- [13]. Y. Yan, C. Li, Z. Li, “Buckling analysis of a 10 MW offshore wind turbine subjected to wind-wave-earthquake loadings” *Ocean Engineering*, Volume 236, 15 September 2021, 109452
- [14]. K. Lin, B. Ma, S. Yang, A. Zhou, “Experimental study of wind turbine in operation under wind and seismic excitations with soil-structure interaction”, *Engineering Structures*, Volume 308, 1 June 2024, 117927
- [15]. N.Mellas, K.Hebbache, A.Mabrouki, M.Mellas, “ A numerical investigation of soil–structure interaction effect on wind turbine behavior under seismic loading”, *Marine Georesources & Geotechnology*, Received 29 Sep 2024, Accepted 07 Jan 2025, Published online: 21 Feb 2025, <https://doi.org/10.1080/1064119X.2025.2460742>

- [16]. Y.Xu, R.Tian, J.Duan, Y.Ding, H.Zhang, “Multi-hazard stochastic response analysis and reliability evaluation of a 5 MW monopile offshore wind turbine based on extended platform FAST-S”, *Engineering Structures*, Volume 305, 15 April 2024, 117674, <https://doi.org/10.1016/j.engstruct.2024.117674>
- [17]. U.Sah, J.Yang, “Importance of higher modes for dynamic soil structure interaction of monopile-supported offshore wind turbines”, *Earthquake Engineering & Structural Dynamics*, Volume 53, Issue 6 May 2024, Pages 1931-2252
- [18]. B.Bozyigit, I.Bozyigit, L.Prendergast, “Analytical approach for seismic analysis of onshore wind turbines considering soil-structure interaction”, *Structures*, Volume 51, May 2023, Pages 226-241, <https://doi.org/10.1016/j.istruc.2023.03.048>
- [19]. A.Karimi, M.Ghanooni-Bagha, E.Ramezani, Ali.Shirzadi Javid, M.Zabihi-Samani “Influential factors on concrete carbonation: a review”, *Magazine of Concrete Research*, Volume 75 Issue 23, December, 2023, pp. 1212-1242, <https://doi.org/10.1680/jmacr.22.00252>
- [20]. P.Guo, H.Ling, Y.Zhang, T.Di, “Modelling of foundation damping in time-domain analysis of monopile supported offshore wind turbine structures”, *Marine Structures*, Volume 98, 2024, 103672, ISSN 0951-8339, <https://doi.org/10.1016/j.marstruc.2024.103672>
- [21]. M.Zabihi Samani, M.Daryabari, A.Daryabari, A.Mirhabibi, “Numerical and Laboratory Investigation of Optimal FIROZBAHRAM soil Improvement with Lime and Cement and Its Impact on Reduction of Soil Settlement in West Tehran Wastewater Treatment Plant”, *Amirkabir J. Civil Eng.*, 53(7) (2021) 645-648
- [22]. A.Chopra, “Dynamics of Structures: Theory and Applications to Earthquake Engineering”, First published (1995)